

Arc-Plasma Wire Spraying: An Optical Study of Process Phenomenology

I.P. Gulyaev, A.V. Dolmatov, M.Yu. Kharlamov, P.Yu. Gulyaev, V.I. Jordan, I.V. Krivtsun, V.M. Korzhyk, and O.I. Demyanov

(Submitted August 17, 2015; in revised form October 30, 2015)

In the present paper, we report on the results of an experimental study of heat- and mass-transfer processes in a Plazer 30-PL-W plasma-jet facility used for arc-plasma wire spraying. Using an original optical diagnostic system, we have studied melting behavior of the metal wire, break up and atomization of liquid metal. For the first time, experimental data on the in-flight velocity and temperature of spray particles in arc-plasma wire spraying were obtained. In spite of moderate particle velocities (about 50 m/s), the obtained steel coatings proved to have a low porosity of 1.5%. While studying the spraying process of tungsten wire, we observed the occurrence of anomalous high-velocity (over 4000 m/s) outbursts ejected from the surface of liquid metal droplets. The nature of such outbursts calls for further study.

Keywords coatings, droplet breakup, optical diagnostics, plasma-arc wire spraying, temperature measurement, velocity measurement

1. Introduction

Presently, thermal spray technologies (Ref 1, 2) are deeply integrated in many industrial manufacturing processes ranging from gas-turbine engines to microelectronics (Ref 3, 4). The choice of the particular thermal spray method (Ref 1, 2, 5-7) (plasma, detonation, HVOF, arc spray, etc.) depend on the type of the material to be sprayed, coatings properties requirements, throughput efficiency and cost of the spraying process and equipment. One of the new thermal spray processes is plasma-arc wire spraying, which features a low cost and high throughput. A specific feature of the method is the use of electric arc both for melting of a feedstock wire (consumable electrode) and for heating of a plasma gas being used for atomization and acceleration of sprayed material (Ref 8, 9). A shielding gas is used to shape the plasma jet and protect it from mixing with ambient atmosphere (Fig. 1). Here, the heating and melting of wire material is due to the heat flux from the plasma flow; due to the heat release at the anode attachment spot of the arc; and due to Joule heating of the wire. Similar to twin-wire arc spray

(TWAS), completely molten metal particles enter the plasma flow and build up a coating.

At its current developmental stage, the plasma-arc wire spraying method just starts being introduced into industry, with its phenomenology and quantitative characteristics having not been adequately understood yet. For instance, the authors of Ref 10, 11 numerically simulated the formation and breaking-up of liquid drops under high-velocity plasma flow over a molten wire tip. Computational characteristics of the particles formed during spraying of steel wire under typical plasma-arc spraying conditions were evaluated. According to the calculations (Ref 11), at a spraying distance of 150 mm, a major part of particles has sizes 40-200 μm (micrometers), the average velocity of the particles being 130-150 m/s, and their average temperature, about 3100-3200 K. The fact that no experimental data characterizing this process have been reported so far in the literature motivated the present study.

At the same time, it should be noted that the melting behavior of wires in TWAS process, which is allied to arc-plasma wire spraying, has been studied in more detail. The structures of liquid metal extrusions, formed at the edges of the electrodes, were categorized in Ref 12. The difference in constricted arc attachment on the cathode and diffuse attachments on the anode leads to asymmetric melting of the wire tips, and the length of the anode liquid sheet increases dramatically with rise of current. Authors of Ref 13 used high-speed camera to observe melting behavior, particle formation and arc movement under different operating conditions of solid and cored wires spraying using Smart Arc 350 PPG system. In particular, it was shown that lower arc current (coupled with lower wire feed rate) leads to shorter length of extruded metal sheets and its regular disintegration (in the form of smaller droplets). In Ref 14, the size distribution of particles from individual wires (copper and steel) was studied for various nozzle geometries of Tafa 9000 spray system. The mass

I.P. Gulyaev, S.A. Khristianovich Institute of Theoretical and Applied Mechanics SB RAS, Novosibirsk, Russia and Yugra State University, Khanty-Mansiysk, Russia; A.V. Dolmatov and P.Yu. Gulyaev, Yugra State University, Khanty-Mansiysk Russia; M.Yu. Kharlamov, I.V. Krivtsun, V.M. Korzhyk, and O.I. Demyanov, E.O. Paton Electric-Welding Institute of the NAS of Ukraine, Kiev, Ukraine; and V.I. Jordan, Altai State University, Barnaul, Russia. Contact e-mail: Gulyaev@itam.nsc.ru.

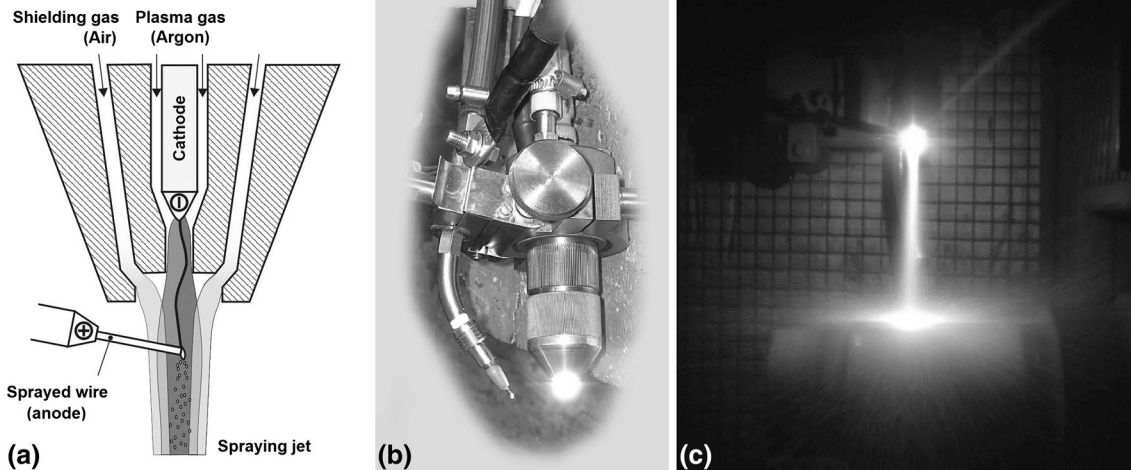
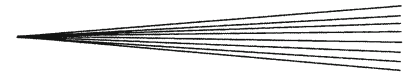


Fig. 1 The PLAZER 30-PL-W plasma-arc spraying facility: (a) schematic diagram of the plasma gun, (b) external appearance of the plasma gun with a wire, (c) coating deposition process

mean values of particles size after complete atomization of 30–50 μm and maximum size below 200 μm were reported. The DPV-2000 optical monitoring system was used in Ref 15 to study aluminum wire spraying process at Valuarc 200 facility. The volumetric mean size of anodic particles was found to be about 180 μm and of cathodic particles was found to be about 120 μm . Velocity of particles decreased with distance from the nozzle, falling from 160 m/s (70 mm downstream) to about 100 m/s (200 mm downstream). Temperature of particles was almost constant (about 2400 K) over the length of the spraying jet. Speaking of the temperature measurements, it is worth to note that all modern diagnostics systems for thermal spray completely rely on the two-color pyrometry method (Ref 16).

2. Experimental

The experiments were performed in Paton Electric-Welding Institute of the NAS of Ukraine (Kiev). In the experiments, a PLAZER 30-PL-W plasma-arc spraying facility was used to spray SV-08 low-carbon steel wire of 1.6-mm diameter and tungsten wire of 2.0-mm diameter. The plasma gas was argon, and the shielding gas was air. The operation conditions examined in experiments are summarized in Table 1.

The heat- and mass-transfer phenomena involved in the plasma-arc wire spraying process were experimentally studied using a specially designed spectral-brightness pyrometry system. This system was developed at Yugra State University (Khanty-Mansiysk, Russia) in collaboration with Institute of Theoretical and Applied Mechanics SB RAS (Novosibirsk, Russia) (Ref 17–19). The pyrometric system comprised a monochrome video channel and a spectral channel (Fig. 2). The former channel was built around an HD1-1312 digital camera (Photon Focus, Switzerland) with 1312×1082 pixels CMOS detector, and was provided with an optical bandpass filter (central

wavelength 575 nm, FWHM 50 nm). The camera provided registration of monochromatic (brightness) images of a two-phase jet at 200-fps rate. Changeable lenses of the digital camera provided a spatial resolution of 22.4 and 51.9 $\mu\text{m}/\text{pixel}$ in the recorded frames. The monochrome video channel was calibrated on an automated bench equipped with a temperature standard—tungsten lamp (Ref 20). In addition, an original approach to the analysis of brightness images of moving objects (tracks) was employed, which has enabled application of the brightness pyrometry method for particle temperature measurements (Ref 20). In the second channel, an LR1-T photospectrometer (Aseq Instr., Canada) was used to register the spectrum of optical emission from the spray jet in 300–900 nm spectral range (resolution 1 nm). Using this spectral information, a spectral region exhibiting no plasma emission lines was selected for video channel and to measure in-flight temperature of metal particles with the independent spectral pyrometry method. The measurement error of the optical diagnostic system for particle velocities was evaluated at a level of 1%, and for particle temperatures, at a level of 2–4% (Ref 21).

The XRD study of the phase composition of sprayed coatings was performed on a D8 Advance (Bruker, Germany) instrument using Cu emission at wavelength 1.5418 Å. The morphology of deposited coatings was studied with Evo MA15 scanning electron microscope (Carl Zeiss, Germany), and the Vickers microhardness study was performed on a DM-8 instrument (Affri, Italy). The sizes of metal particles were determined by spraying particles into water, collecting them and studying with LS1320 (Beckman Coulter, USA) laser diffraction size analyzer.

3. Visualization of the Spray Process

The general structure of the two-phase flow in the plasma-arc spraying process is illustrated in Fig. 3. This

Table 1 Plasma-arc wire spraying facility operation regimes

No.	Arc current, A	Arc voltage, V	Plasma gas (argon) flow rate, l/min	Shielding gas (air) flow rate, l/min	Wire feed rate, m/min	Inter-electrode distance, mm
Steel wire 1.6 mm						
1	220	65...70	28	330	6.3	9
2	260	65...70	28	330	9.3	9
3	300	65...70	28	330	15.5	9
Tungsten wire 2.0 mm						
4	300	70	25	330	15	7

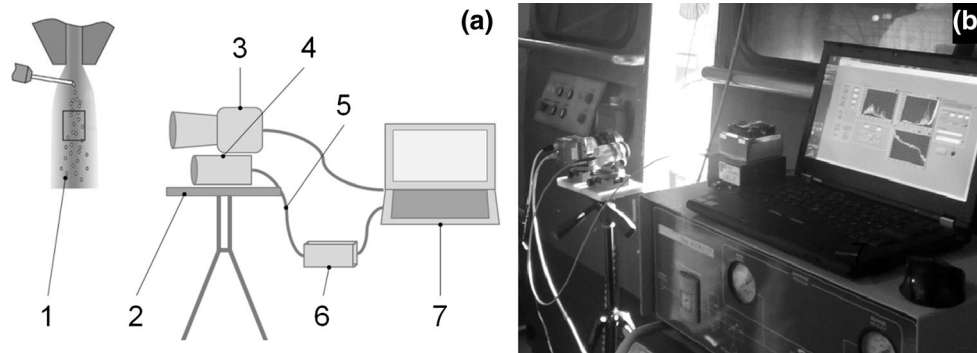


Fig. 2 The spectral-brightness optical diagnostic system: (a) schematic diagram, (b) external appearance of the system during operation of the spraying facility. 1—two-phase plasma jet, 2—adjustable tripod-mounted platform, 3—camera, 4—photospectrometer lens, 5—optical fiber, 6—photospectrometer, 7—laptop

figure shows reconstruction of the spray jet 0-16 cm length for operation regime #1 in the table: 1.6-mm steel wire at arc current 220 A. The reconstructed image merges individual particle tracks that were identified in multiple video frames. The spraying spot has a diameter of 4 cm at a distance of 16 cm, and the intensive atomization of particles takes place at a distance of 30 mm from the wire tip (~40 mm from the nozzle). These data fairly well agree with the calculation results of Ref 11.

Considering specific features of the plasma-arc spraying method, it is of interest to examine the melting behavior of the conducting wire in the electric-arc attachment spot. Video frames of this process obtained in spraying 1.6-mm diameter steel wire are shown in Fig. 4. Here, the arc ignition in the regime with 260-A arc current is shown: the wire has not been melted yet, and the electric arc coming out of plasma-gun nozzle and attaching to the wire tip can be seen.

The atomization process of liquid metal at 260-A arc current is illustrated in Fig. 4(b). Under the dynamic pressure due of the plasma flow, the melt forms a liquid sheet. At the contact with the wire, the diameter of the liquid sheet 300 μm decreases to 100-200 μm in downstream direction. At a distance of 3.5-4 mm from the wire tip, the liquid sheet gets atomized predominantly into drops sized 100 to 200 μm . Further drop atomization proceeds outside the filmed zone. The formation process of molten drops at 220-A arc current is shown in Fig. 4(c). In the latter case, no liquid sheet is formed at the anode wire; instead, large drops of 300-600 μm size are come off

the wire tip. Due to their inertia, the large drops undergo slow acceleration, and they reside in the high-temperature zone of the plasma flow over a long time, which leads to an intensive evaporation of the liquid drop and the metal vapor can be distinctly seen on the downwind side of the droplet. Figure 4(d) shows the formation of fine molten droplets at the wire tip at 300-A arc current operation. A large number of small particles with sizes below 100 μm are formed, which can be a result of turbulent flow across the wire tip at raised flow velocity. It is worth to note that rise of the arc current from 220 to 300 A did not increase the anodic sheet length, as it was observed in Ref 12.

Application of the spectral channel of the diagnostic system has allowed us to register the integral emission of the two-phase jet that involved the thermal emission from metal particles (continuous spectrum) and the background emission due to plasma (for the main part, line spectrum). The optical emission spectra of the jet registered at various distances from the nozzle edge are shown in Fig. 5. Evidently, the line emission due to plasma is predominantly concentrated in two spectral regions, 350 to 500 nm (Ar^+ ions) and 650-1000 nm (neutral Ar atoms) (Ref 22). For this reason, optical bandpass filter with CWL 575 nm was used for the video channel of the diagnostic system. Moreover, the continuous spectrum observed in the spectral region from 550 to 600 nm has allowed us to perform particle temperature measurements by the spectral pyrometry method (Ref 23-25). It is a well-known fact (see, e.g., Ref 26) that, in measuring the thermal emission from the surface of a non-uniformly heated object, the

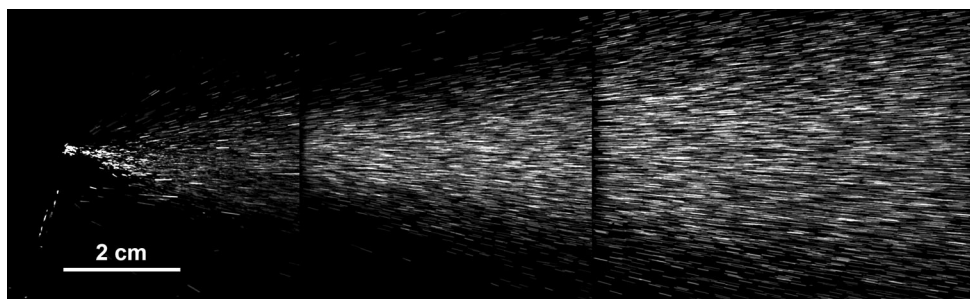


Fig. 3 Reconstructed image of the two-phase jet in plasma-arc wire spraying. 1.6-mm steel wire, 220 A

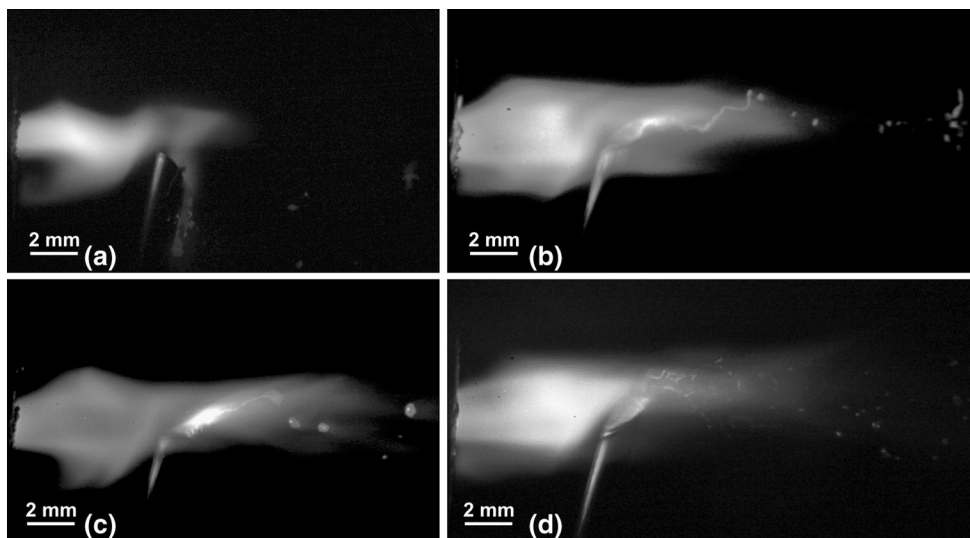


Fig. 4 Visualization of the 1.6-mm-diameter steel wire melting and drops atomization process: (a) arc ignition (260 A); (b) fragmentation of liquid sheet (260 A); (c) formation of large drops (220 A); (d) formation of fine drops (300 A)

spectral method yields a temperature value close to the maximum temperature in the observation region. The latter statement is valid providing that surface of the high-temperature region on the object is not too small.

The size distribution of solid particles obtained by quenching liquid drops in water at a distance of 200 mm from the plasma-gun nozzle is shown in Fig. 6. In contrast to powder spraying methods, here the range of particle sizes is perfectly wide, 400 nm to 400 μm , due to the intense fractionation and evaporation process of liquid particles proceeding over the initial length of the plasma jet. Although a main number of the particles had rather small sizes (less than 2-3 μm) their mass fraction was negligibly small. The following two facts important for practice deserve to be mentioned: (1) a predominant mass fraction of the particles forming a coating was sized 50-400 μm ; (2) the total surface area of particles was uniformly distributed among the drops whose sizes ranged from 500 nm to 200 μm ; hence, it can be argued that spectral pyrometry temperature results correspond to the hottest spray particles in the jet. Over the initial length of the jet, where the plasma flow temperature is high (up to 11,000 K), the hottest one is the fine particle fraction,

which instantly acquire the temperature of the plasma flow and, in this way, serve the “markers.” Farther downstream, where the plasma temperature gradually decreases, the hottest one is the coarse particle fraction, which undergo a rather slow cooling as they leave the jet.

4. Measurement of Particles In-Flight Velocity and Temperature

Results of velocity and temperature measurements of molten drops performed with the help of the video channel of the diagnostic system are shown in Fig. 7. The employed image processing algorithm permitted identification of particles larger than 50 μm in diameter (Ref 21, 27).

The average velocity of particles as a function of the distance to the plasma torch nozzle for three different regimes of steel-wire spraying (arc currents 220, 260, and 300 A) is shown in Fig. 7(a). Evidently, in all the three cases, the highest average velocity of spray particles is at the level of 45 m/s, the latter value being lower than the

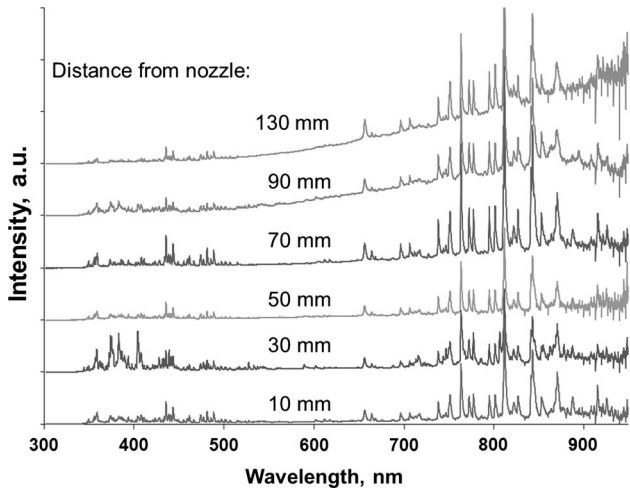


Fig. 5 Emission spectra of the two-phase plasma jet measured at various distances from the nozzle edge

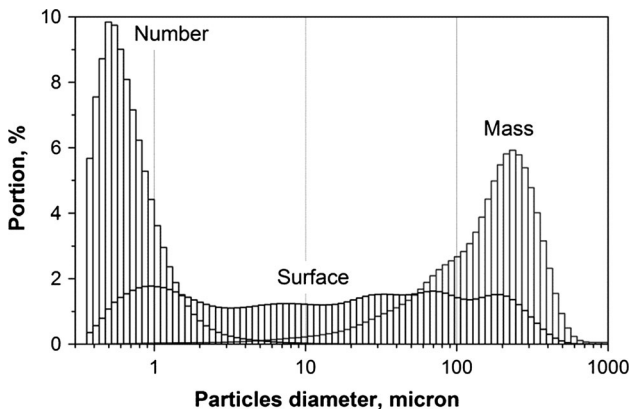


Fig. 6 The size distribution of particles in spraying 1.6-mm steel wire (260 A)

estimate obtained by numerical simulations in the paper (Ref 11). Particles are intensively accelerated in the initial region of the jet. For the arc currents 220 and 260 A, this region has a length of 7 cm, and for the arc current 300 A, about 11 cm. The mentioned initial region corresponds to the core of the jet flow, that is, to the region in which both the velocity and temperature of the plasma flow have highest values. The dependence of the average particle temperature under the same spraying conditions is shown in Fig. 7(b). Here, the length of the jet core is estimated to be 7 cm for arc currents 220 and 260 A, and 12 cm for the arc current 300 A. The latter values well agree with estimates based on particles velocity dynamics. A sharp rise of average particle temperature (approximately 180 K) over a distance of 12 cm under conditions with the arc current 260 A is due to the change of filming conditions in the jet flow region 12 to 16 cm from the nozzle exit (diagnostic equipment displacement). At the currents 220 and 260 A, the particle temperature attains its highest value of about 2750 K; the maximum particle temperature at 300 A arc

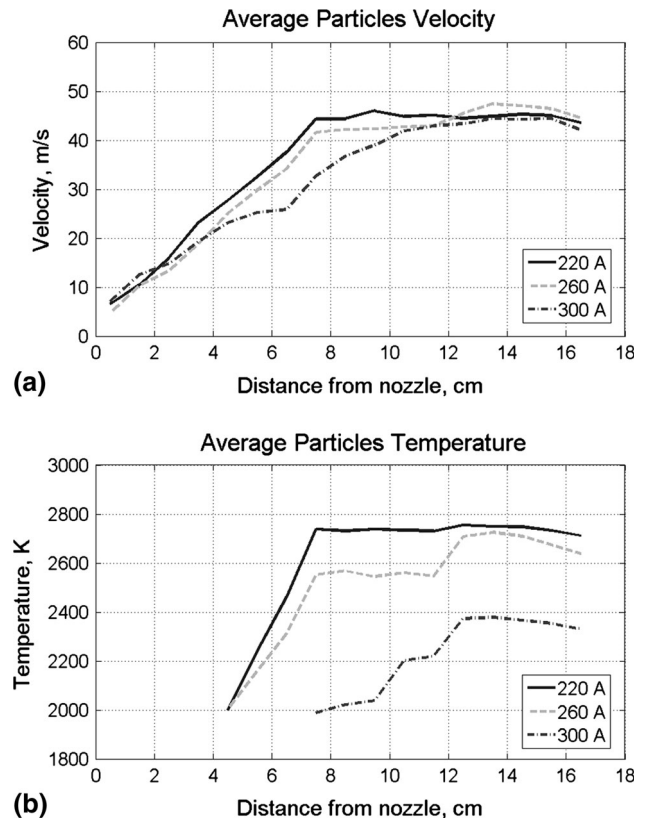


Fig. 7 Measured in-flight particles parameters as a function of a distance from nozzle at various arc currents: (a) average velocity, (b) average temperature

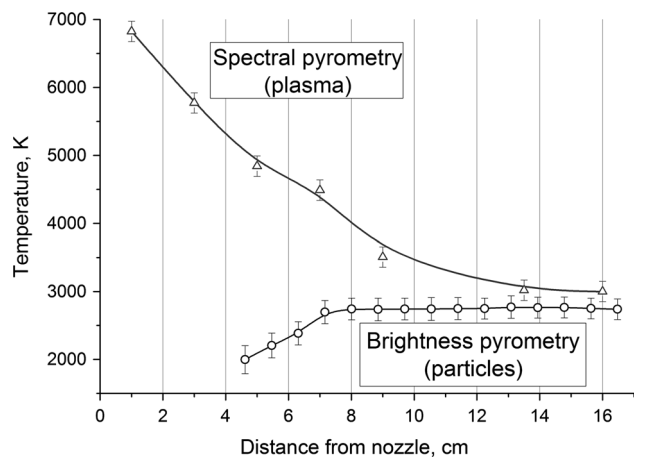


Fig. 8 Temperature measurement results obtained by the spectral and brightness pyrometry methods. 220 A arc current

current is much lower, about 2400 K. It is worth to note that the measured temperatures are 300-600 K below the calculated values of Ref 11. The optimal spraying conditions corresponding to maximum particle velocities and temperatures for 1.6 mm steel wire were determined to be: 220 A arc current, spray distance 14 to 16 cm.

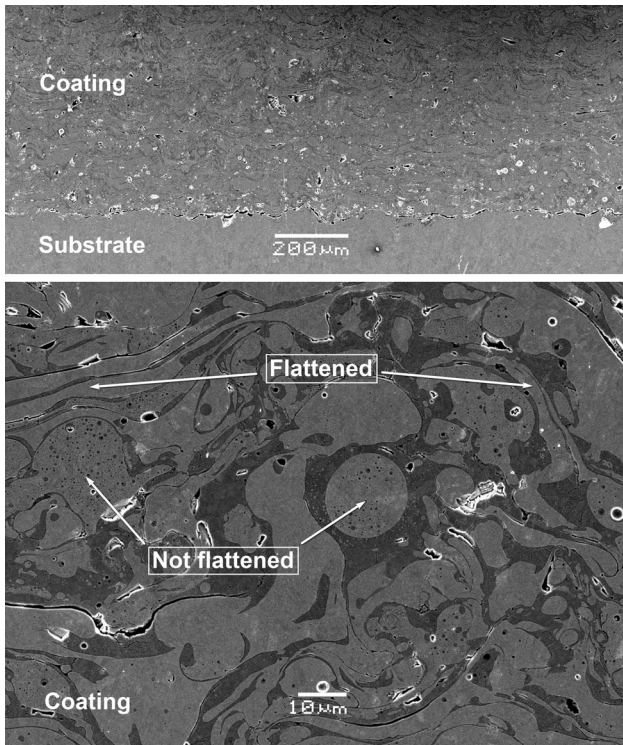
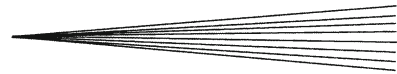


Fig. 9 Cross section of a steel coating sprayed at 220 A arc current (SEM image)

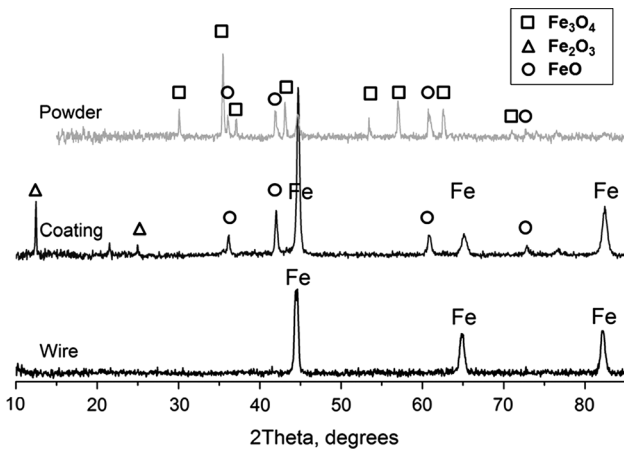


Fig. 10 XRD patterns of the initial steel wire, the deposited coating, and the water-quenched powder

It is of interest to compare results of temperature measurements conducted using spectral pyrometry and brightness pyrometry methods; such a comparison is given in Fig. 8. Evidently, the “spectral” temperature monotonically decreases from 7000 K in the vicinity of the nozzle to approximately 3000 K at a distance of 14-16 cm from the nozzle exit. We believe that the latter dynamics reflects the variation of local plasma temperature. Markers that acquire the flow temperature and increase the optical density (and emissivity) of the two-phase flow are the sub-micron particles (see Fig. 6) and metal vapor.

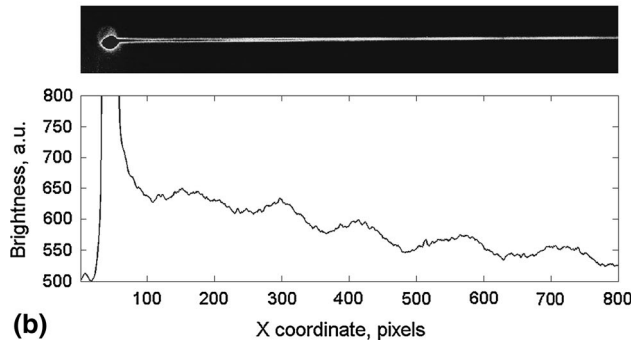
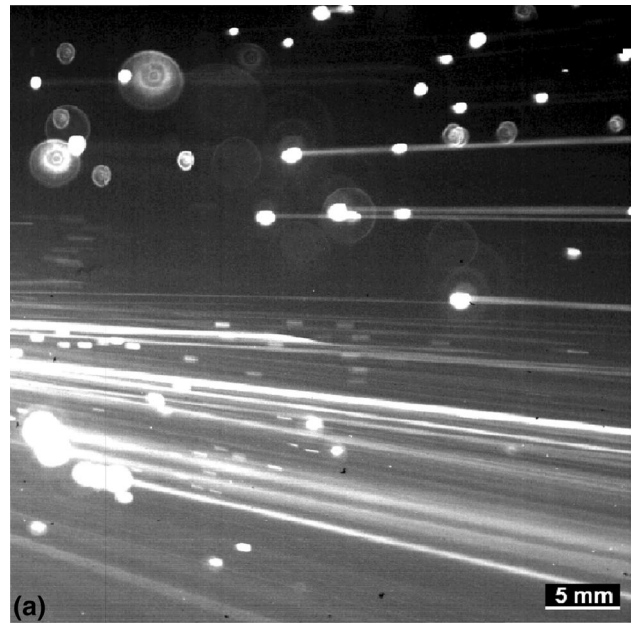


Fig. 11 Anomalous high-velocity outbursts from the surface of tungsten drops: (a) single frame of the two-phase jet. Width of the frame 42 mm, exposure time 10 μs, (b) an individual outburst extracted from the video-frame and the distribution of brightness along length of its track

Farther from the nozzle, the obtained “spectral” and “brightness” temperatures approach each other to become nearly equal at a level of 2800-3000 K. Farther downstream, the gas flow gets cooled down more quickly than the spray particles do, and the temperature results obtained by the both pyrometric methods correspond to the temperature of large particles over 50 μm.

5. Sprayed Coatings

The 1.6-mm steel wire was used to deposit coating samples onto St-3 steel substrates in operation regime #1: arc current 220 A, spraying distance 160 mm. The cross section of 800-μm-thick deposited coating is shown in Fig. 9. In spite of comparatively low particle velocities in the jet, the coatings here have a dense structure. The porosity measured by SEM image analysis method was found to be 0.85-1.5%. Such low values of coating poros-

ity, normally typical for high-velocity spraying methods such as HVOF or detonation spraying, can be attributed to an absence of unmelted particles in the spray jet. As one can see in lower part of Fig. 9 the coating doesn't have typical laminar structure formed by flattened particles—splats. Considerable amount of not flattened (spherical or partially deformed) particles of 15-25 μm size presents in the deposit. This could be attributed to substantial deceleration of these small drops in the gas boundary layer on the substrate surface. Also these small, not flattened particles exhibit signs of boiling—numerous fine pores of size below 1 μm . In plasma spray this effect often takes place as fine powder fraction gets overheated in a plasma jet core.

Figure 10 presents the XRD patterns of the initial wire, the surface of deposited coating, and the particles sprayed into water to measure their size (see Fig. 6). The diffraction pattern of the initial wire material contains peaks iron (Fe) only, whereas the coating material exhibits a small amount of FeO and Fe₂O₃ resulting from the partial oxidation of the spray material. The pattern of spherical powder particles predominantly demonstrates peaks of FeO, Fe₂O₃, and Fe₃O₄ oxides that were intensively produced on the surface of incandescent drops interacting with water. The measured surface hardness of coating is 700 HV.

6. Anomalous High-Velocity Outbursts Observed in Tungsten Spraying

The spraying of 2-mm-tungsten wire was investigated (regime #4). This study has revealed a few anomalous effects. An image of the spray jet region 7-11 cm from the plasma gun nozzle (here, the flow moves from left to right) is shown in Fig. 11. It is seen that, around many tungsten particles, there form radiating spheres with diameters up to 5 mm. Such particles were the cause of high-velocity outbursts ejected along the direction of two-phase plasma flow. In the same frame, ordinary metal-drop tracks of length 0.5-1 mm, which values correspond to velocities 50-100 m/s, are seen. The presence of outbursts whose tracks cross the whole frame indicate that the velocity of such outbursts exceeds 4200 m/s (width of the frame is 42 mm, exposure time 10 μs). An image of an individual radiating particle and the distribution of emission intensity along a high-speed outburst are shown in Fig. 11(b). Here, the brightness exhibits a decaying wavy pattern with a wavelength of 5-8 mm. In the examined emission spectrum of the two-phase plasma jet, no anomalous lines or substantial differences from the spectra of Fig. 5 were revealed.

Presently, the nature of the observed phenomenon remains unclear. However, we believe that this phenomenon is related with the high melting temperature of tungsten (3700 K), which leads to raised thermionic emission of electrons. As a result, a region with spatial separation of charges (negative electron cloud and positive metal particle) may form, and this may lead to gas discharge similar to corona (Ref 28).

7. Conclusions

The present study performed using original optical diagnostics system has allowed us to investigate a plasma-arc wire spraying process at PLAZER 30-PL-W facility. The formation of liquid metal sheets and drops atomization was visualized and effect of arc current was investigated. The in-flight velocity and temperature of particles, and their size distribution, were evaluated. The produced steel coatings demonstrated porosity below 1.5% in spite of relatively low particle-velocity values. The obtained results provide the basis for advance in design of the spraying equipment and experimental data for verification of mathematical models of molten metal droplets motion, heating, and breakup in the plasma jet.

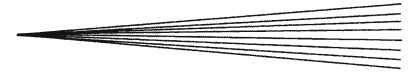
An unexpected effect, namely, the formation of anomalous outbursts with velocities in excess of 4000 m/s, was observed in tungsten spraying experiments. The nature of this phenomenon calls for further study.

Acknowledgment

This work was supported by the Russian Foundation for Basic Research (Projects 14-08-90428 and 15-48-00100) and by the Ukrainian National Academy of Sciences (Project 06-08-14).

References

1. L. Pawlowski, *Science and Engineering of Thermal Spray Coatings*, 2nd ed., Wiley, Chichester, 2008, p 656
2. J.R. Davis, Ed., *Handbook of Thermal Spray Technology*, ASM International, Materials Park, OH, 2004
3. K.E. Schneider, V. Belashchenko, M. Dratwinski, S. Siegmann, and A. Zagorski, *Thermal Spraying for Power Generation Components*, Wiley, Weinheim, 2007, p 271
4. S. Sampath, Thermal Spray Applications in Electronics and Sensors: Past, Present and Future, *J. Therm. Spray Technol.*, 2009, **19**(5), p 921-949
5. S. Lima and B.R. Marple, Thermal Spray Coatings Engineered from Nanostructured Ceramic Agglomerated Powders for Structural, Thermal Barrier and Biomedical Applications: A Review, *J. Therm. Spray Technol.*, 2007, **16**(1), p 40-63
6. W. Tillmann, E. Vogli, I. Baumann, B. Krebs, and J. Nebel, Wear-Protective Cermet Coatings for Forming Tools, *Mater. Werkst.*, 2010, **41**(7), p 597-607
7. V. Uliantisky, A. Shtertser, S. Zlobin, and I. Smurov, Computer-Controlled Detonation Spraying: From Process Fundamentals Toward Advanced Applications (Review), *J. Therm. Spray Technol.*, 2011, **20**(4), p 791-801
8. M.Yu. Kharlamov, I.V. Krivtsun, V.N. Korzhik, and S.V. Petrov, Formation of Liquid Metal Film at the Tip of Wire-Anode in Plasma-Arc Spraying, *Paton Weld. J.*, 2011, **12**, p 2-6
9. I.P. Gulyaev, P.Y. Gulyaev, V.N. Korzhik, A.V. Dolmatov, V.I. Iordan, I.V. Krivtsun, M.Y. Kharlamov, and A.I. Demyanov, An Experimental Study of the Plasma-Arc Wire Spraying Process, *Paton Weld. J.*, 2015, **3**(4), p 36-41
10. M.Yu. Kharlamov, I.V. Krivtsun, and V.N. Korzhik, Dynamic Model of the Wire Dispersion Process in Plasma-Arc Spraying, *J. Therm. Spray Technol.*, 2014, **23**(3), p 420-430
11. M.Yu. Kharlamov, I.V. Krivtsun, V.N. Korzhik, Y.V. Ryabovolyk, and O.I. Dem'yanov, Simulation of Motion, Heating, and Breakup of Molten Metal Droplets in the Plasma Jet at Plasma-Arc Spraying, *J. Therm. Spray Technol.*, 2015, **24**(4), p 659-670



12. N.A. Hussary and J.V.R. Heberlein, Atomization and Particle-Jet Interactions in the Wire-Arc Spraying Process, *J. Therm. Spray Technol.*, 2001, **10**, p 604-610
13. W. Tillmann and M. Abdulgader, Wire Composition: Its Effect on Metal Disintegration and Particle Formation in Twin-Wire Arc-Spraying Process, *J. Therm. Spray Technol.*, 2013, **22**(2-3), p 352-362
14. H.L. Liao, Y.L. Zhu, R. Bolot, C. Coddet, and S.N. Ma, Size Distribution of Particles from Individual Wires and the Effects of Nozzle Geometry in Twin Wire Arc Spraying, *Surf. Coat. Technol.*, 2005, **200**, p 2123-2130
15. A. Pourmousa, J. Mostaghimi, A. Abedini, and S. Chandra, Particle Size Distribution in a Wire-Arc Spraying System, *Therm. Spray Technol.*, 2005, **14**(4), p 502-510
16. G. Mauer, R. Vaßen, and D. Stover, Plasma and Particle Temperature Measurements in Thermal Spray: Approaches and Applications, *Therm. Spray Technol.*, 2011, **20**(3), p 391-406
17. Patent Pending, A Method of Spectral-Brightness Pyrometry of Objects with a Non-Uniform Surface Temperature, Russian Federation No. 2015123313, 17 June 2015
18. P.Yu. Gulyaev, H. Cui, I.P. Gulyaev, and I.V. Milyukova, Temperature Measurements for Ni-Al and Ti-Al Phase Control in SHS Synthesis and Plasma Spray Processes, *High Temp. High Press.*, 2015, **44**(2), p 83-92
19. K.A. Ermakov, A.V. Dolmatov, and I.P. Gulyaev, A system for Optical Diagnostics of Particle Velocity and Temperature in Gas-Thermal Spraying Processes, *Bull. Yugra State Univ.*, 2014, **33**(2), p 56-68 [in Russian]
20. A.V. Dolmatov, K.A. Ermakov, V.V. Lavrikov, and A.O. Makoveev, An Automated Complex for Calibration of Thermography Systems Based on the MATLAB Software, *Bull. Yugra State Univ.*, 2012, **25**(2), p 59-63 [in Russian]
21. M.P. Boronenko, I.P. Gulyaev, P.Y. Gulyaev, A.I. Demyanov, A.V. Dolmatov, V.I. Iordan, V.N. Korzhik, I.V. Krivtsun, and M.Yu. Kharlamov, Estimate of Dispersed Phase Velocity and Temperature in Plasma-Arc Spraying Jets, *Fundam. Res.*, 2014, **11**(10), p 2135-2140 [in Russian]
22. Strong lines of Argon (Ar), <http://physics.nist.gov/PhysRefData/Handbook/Tables/argontable2.htm>
23. A.N. Magunov, The Choice of a Spectral Interval Within Which a Heated Opaque Object Radiates as a Gray Body, *Instrum. Exp. Tech.*, 2010, **53**(6), p 910-914
24. A.V. Dolmatov, I.P. Gulyaev, and R.R. Imamov, A Spectral Pyrometer for the Control of Temperature in Thermal Synthesis Processes, *Bull. Yugra State Univ.*, 2014, **33**(2), p 32-42 [in Russian]
25. I.P. Gulyaev, K.A. Ermakov, and P.Yu. Gulyaev, New High-Speed Combination of Spectroscopic and Brightness Pyrometry for Studying Particles Temperature Distribution in Plasma Jets, *Eur. Res.*, 2014, **71**(3-2), p 564-570
26. A.N. Magunov, Spectral Pyrometry of Objects with a Nonuniform Temperature, *Tech. Phys. Russ. J. Appl. Phys.*, 2010, **55**(7), p 991-995
27. A.V. Dolmatov, I.P. Gulyaev, and V.I. Jordan, The Optical Control System of Dispersed Phase Properties in Thermal Spray Process, *IOP Conf. Ser. Mater. Sci. Eng.*, 2015, **81**, p 012041
28. Y.P. Raiser, *Gas Discharge Physics*, Springer, Berlin, 1991, p 449